Polymer 50 (2009) 5720–5727

Contents lists available at ScienceDirect

Polymer

journal homepage: www.elsevier.com/locate/polymer

# Counterion motions and thermal ordering effects in perfluorosulfonate ionomers probed by solid-state NMR

Jong Keun Park, Justin Spano, Robert B. Moore, Sungsool Wi*

*Department of Chemistry, Virginia Polytechnic Institute and State University, Blacksburg, VA 24061, USA*

ARTICLE INFO

*Article history:*
Received 2 October 2009
Accepted 6 October 2009
Available online 12 October 2009

*Keywords:*
Solid-state NMR spectroscopy
Tetraalkylammonium ion-form perfluorosulfonate ionomers (PFSIs)
Small-angle X-ray scattering (SAXS)

ABSTRACT

Perfluorosulfonate ionomers (PFSIs) neutralized by tetraalkylammonium ions have been investigated using variable temperature $^{1}H$ and $^{13}C$ solid-state NMR (ssNMR) spectroscopy to probe the thermally induced properties of tetraalkylammonium ions at temperatures near the α-relaxations. Tetramethylammonium ($TMA^+$), tetraethylammonium ($TEA^+$), tetrapropylammonium ($TPA^+$) and tetrabutylammonium ($TBA^+$) ions have been incorporated in our study for the systematic control of ionic interactions within PFSIs according to the chain-length of ammonium ions. $^{13}C$ static ssNMR results show that bulkier $TPA^+$ and $TBA^+$ ions undergo molecular tumbling motions near or above the α-relaxation temperature of the corresponding PFSI ionomers, with jumping rates of $\kappa \approx 1$ kHz. Moreover, the results of $^{1}H$ spin-lattice ($T_1$) relaxation time measurements suggest that smaller $TMA^+$ ions in the PFSI exhibit a thermally induced ordering effect as the sample temperature approaches the α-relaxation temperature of $TMA^+$–PFSI. This ordering phenomenon is also supported by the results from small-angle X-ray scattering.



## 1. Introduction

With greater system efficiencies and environmental benefits, proton-exchange membrane electrolyte fuel cells (PEMFCs) have become an attractive system as an alternative to nonrenewable, traditional energy sources. Currently, perfluorosulfonate ionomers (PFSIs), particularly Nafion®, are the benchmark proton-exchange membranes due to their unique morphology, chemical stability, and excellent transport properties [1]. Nafion®, having the chemical structure shown below, is a copolymer of tetrafluoroethylene and generally less than 15 mol% of perfluorovinylether units terminated with sulfonic acid functionalities.

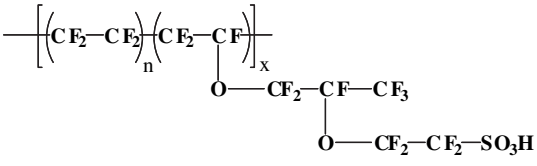


With a sufficient length of polytetrafluoroethylene (PTFE) segments between side-chains, Nafion® is capable of organizing into crystalline domains that are generally less than ca. 10 wt% in 1100 eqivalent weight of Nafion® (EW, the grams of dry polymer per equivalent of sulfonic acid units) [1]. Greater efforts, however, have been given to the unique nanophase-separated morphology observed upon aggregation of the polar, ionic side-chains within the matrix of hydrophobic PTFE. These ionic clusters, and specifically their shape, spatial distribution, and connectivity, precisely define the supramolecular organization and function of this technologically important material as an ionic conductor.

Recognizing the complex nature of the Nafion® morphology, numerous structural models have been proposed based mostly on small-angle X-ray and neutron scattering studies. Hsu and Gierke suggested swollen inverse micelles of roughly spherical geometry that are connected by nanoscale hydrophilic channels concurrent with the unique transport properties exhibited by PFSIs [2]. In addition to the early work of Hsu and Gierke, the most common ones include the core-shell model by Fujimura et al. [3], the local order model by Dreyfus et al. [4], the rod-like aggregate model by Rubatat and coworkers [5], the fringed-micelle model by Kim et al. [6], and most recently, parallel cylindrical water channel model by Schmidt-Rohr [7]. Although each model differs significantly in the shape and order of ionic domains, they all recognize the presence of ionic aggregates that are dispersed throughout the PTFE matrix.

It has been shown that ionic aggregates in PFSIs can act as multifunctional physical cross-links that significantly restrict chain mobility [8,9]. However, the motional constraint imposed by ionic clustering in PFSIs may be weakened by hydration processes and/or control of electrostatic interactions. Page et al. showed that the

* Corresponding author. Tel.: +540 231 3329; fax: +540 231 3255.
*E-mail address:* sungsool@vt.edu (S. Wi).

0032-3861/$ – see front matter © 2009 Elsevier Ltd. All rights reserved.
doi:10.1016/j.polymer.2009.10.016

strength of Columbic interactions within the ionic domain can effectively be manipulated by varying the size of neutralizing counterions, such as $Na^+$, tetramethylammonium ($TMA^+$), tetraethylammonium ($TEA^+$), tetrapropylammonium ($TPA^+$), and tetrabutylammonium ($TBA^+$) ions [10–12]. Dynamic mechanical analysis (DMA), and small-angle X-ray scattering (SAXS) analysis have revealed that tetraalkylammonium ion neutralized PFSIs exhibit two distinct thermo-mechanical relaxations in the range of 70–300 °C that have been assigned as the β- and α-relaxations [1,10]. The α-relaxation temperatures of $TMA^+$–, $TEA^+$–, $TPA^+$– and $TBA^+$–PFSIs are 240 °C, 160 °C, 130 °C, and 100 °C, respectively. On the other hand, the β-relaxation temperatures of $TMA^+$–, $TEA^+$–, $TPA^+$–, and $TBA^+$–PFSI membranes are 130 °C, 111 °C, 100 °C, and 73 °C, respectively [10]. Compared to the sulfonic acid form of the polymer, small $TMA^+$ ions cause dramatic increases in both the $\alpha$ and $\beta$ relaxation temperatures due to the great strength of the electrostatic interactions between the ion-pairs, while larger $TPA^+$ or $TBA^+$ counterions cause the $\alpha$- and $\beta$-relaxations to systematically shift to significantly lower temperatures [10,11,13]. As the size of the counterion increases, the larger counterions significantly weaken the strength of the electrostatic interactions and the bulky, organic counterions can effectively plasticize the ionomer, which in turn yields lower $\alpha$- and $\beta$-relaxation temperatures [10–12]. More specifically, the low temperature $\beta$-relaxation, which is assigned to the genuine $T_g$ of Nafion®, is associated with the onset of thermally activated chain motions (primarily the backbone motions), within the framework of an electrostatically croslinked network [10]. However, the onset of long-range mobility of both the main- and side-chains facilitated by a significant destabilization of the electrostatic network has been assigned to motions associated with the high temperature α-relaxation [10].

To gain a fundamental insight into the thermomechanical behavior, ionic motions, and morphological transformations within these complex materials, solid-state NMR (ssNMR) sprctroscopy is recognized as a powerful method for probing site-specific, molecular dynamics. ssNMR spectroscopy has been widely used for investigating the characteristics of segmental movements of the chain and side-groups in polymers by monitoring the time-dependent, anisotropic NMR frequencies of specific nuclear sites of interest [14–19]. Variable temperature $^{19}F$ chemical shift anisotropy (CSA) measurements have been used to determine the degree of crystallinity and investigating macromolecular motions in PTFE-like backbone [20]. $^{19}F$ and $^{13}C$ CSAs, as well as $^{19}F$–$^{13}C$ dipolar couplings, have been utilized to probe fast, large-amplitude dynamics of both backbone and side-chain segments in Nafion® at ambient temperature [21]. On the basis of the observed counterion effects in Nafion®, Page and coworkers employed $^{19}F$ ssNMR spectroscopy to explore the influence of electrostatic interactions on the local and global chain dynamics in Nafion® samples that are neutralized with $Na^+$, $TMA^+$, and $TBA^+$ [12].

A fundamental understanding of the link between the morphology of PFSIs and their thermomechanical properties can be obtained by investigating the structural organization and molecular motions of the ionic species within the ionic aggregates as a function of counterion size and temperature. In this study, the variable temperature $^1H$ spin-lattice relaxation time, $T_{1,}$ of tetraalkylammonium ions within the ionic domains of PFSIs is measured over temperatures ranging from 24 to 190 °C. Because the spin-lattice relaxation time is governed by high-frequency motions in the order of tens or hundreds of MHz (usually associated with local motions of atoms or molecular segments near the nucleus under investigation [22]), the information obtained from this study will help to better understand the local order origins of the thermomechanical relaxations of tetraalkylammonium-form PFSIs. To further explore the effect of ion size, electrostatic interactions, and ion-pair packing in the aggregates on the counterion mobility, we have also employed variable temperature static $^{13}C$ ssNMR spectroscopy to probe counterion dynamics on the molecular-level.

## 2. Experimental

### 2.1. Materials

The perfluorosulfonate ionomer, Nafion® 117CS membranes (1100 g/equivalent, 7 mil thickness) were purchased from E.I. Dupont de Nemours & Co. and cleaned by refluxing in 8 M nitric acid for 2 h, and then in deionized (DI) water for 1 h. These PFSI samples were then completely neutralized to contain tetramethylammonium ($TMA^+$), tetraethylammonium ($TEA^+$), tetrapropylammonium ($TPA^+$), and tetrabutylammonium ($TBA^+$) counterions by soaking the $H^+$-form membranes in excess (ca. 5×) methanolic or aqueous solution of the appropriate alkylammonium hydroxide. The neutralized membranes were thoroughly rinsed of excess alkylammonium hydroxide and dried in a vacuum oven at 70 °C overnight.

### 2.2. NMR spectroscopy

The NMR experiments were performed on a Bruker Avance II-300 wide-bore NMR spectrometer (7.05 T) operating at Larmor frequencies of 75.47 MHz for $^{13}C$ and 300.13 MHz for $^1H$ nuclei. Static $^{13}C$ ssNMR spectra of tetraalkylammonium ions bound in the ionic domains of PFSI membranes were acquired by employing a cross-polarization (CP) sequence shown in Fig. 1A. The NMR signal averaging for $^{13}C$ spectral acquisition was achieved by co-adding 4096 transients with a 5 s acquisition delay time. An inversion recovery method [23], implemented with a static CP-based $^{13}C$-detection scheme (Fig. 1B), was incorporated to measure the $T_1$ relaxation times of the methylene or methyl protons adjacent to the nitrogen atoms of the alkylammonium ions. The proton $T_1$ relaxation of tetraalkylammonium ions was detected indirectly via the $^{13}C$ signals, incorporating a short one-bond $^1H$–$^{13}C$ Lee–Goldburg cross-polarization (LGCP) [24,25] (~150 μs) transfer as shown in Fig. 1B. Proton equilibrium magnetizations are inverted by a 180° pulse, followed by a variable delay time, $\tau$, and consecutively

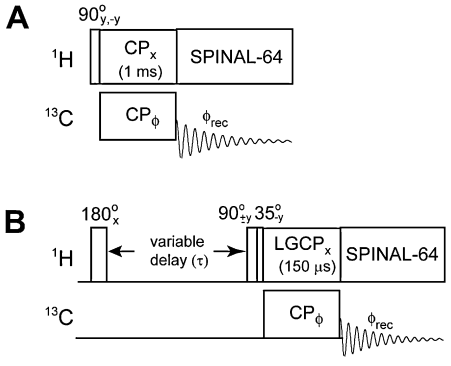


**Fig. 1.** The pulse sequences used in our experiments for obtaining $^{13}C$ static CP spectra (A) and $^1H$ $T_1$ s (B). A CP mixing time of 1 ms was applied for obtaining $^1H$–$^{13}C$ polarization transfer with a 2 s acquisition delay (A). A variable delay time $\tau$ following the initial 180 degree pulse was allowed for measuring $T_1$ of protons in alkylammonium ions, which are monitored indirectly via the $^{13}C$ signals of the directly bonded $^{13}C$ nuclei, obtained using a short (~150 μs) LGCP scheme for selective detection (B). The pulse phase $\phi$ and the signal acquisition phase $\phi_{rec}$ in both sequences are: $\phi = x, x, y, y, -x, -x, -y, -y$; $\phi_{rec} = x, -x, y, -y, -x, x, -y, y$.

detected by a 90° read pulse. This read pulse was combined with a LGCP scheme for signal encoding along the directly bonded $^{13}C$ sites. The NMR signal averaging for $^{1}H$ $T_1$ measurement was achieved by co-adding 4096 transients with a 10 s acquisition delay time. The sample temperature in the NMR probe was regulated by an air flow, which was under the control of a BVT-3000 digital temperature control unit of a Bruker console and a BCU-X precooling and stabilization accessory. The sample temperatures used in our NMR experiments were 24 °C, 40 °C, 80 °C, 120 °C, 160 °C, and 190 °C for acquiring static $^{13}C$ NMR spectra, and 24 °C, 120 °C, and 190 °C for measuring the $^{1}H$ $T_1$ relaxations. $^{1}H$ $\pi/2$ and $\pi$ pulse lengths were 4.5 and 9 μs, respectively. The SPINAL-64 decoupling sequence [26] at 62.5 kHz power was used for proton decoupling during $^{13}C$ signal detection.

### 2.3. Small-angle X-ray scattering (SAXS)

Synchrotron small-angle X-ray scattering (SAXS) experiments were performed at Station 4C1 of the Pohang Accelerator Laboratory (PAL) (Pohang, Korea). The incident X-ray beam was tuned to a wavelength of 1.30 Å and the sample-to-detector distance was 1075 mm. The two-dimensional scattering images were recorded using a Mar CCD camera with 30 s exposure time. The relationship between pixel and the momentum transfer vector q was determined by calibrating the scattering data with a silver behenate standard. All scattering intensities were corrected for transmission, incident beam flux, and background scatter due to air and Kapton windows. The $TMA^+$ and $TBA^+$-form membranes were annealed at 150 and 200 °C for 10 min and then cooled to room temperature prior to SAXS experiments.

### 2.4. Dynamic solid-state NMR lineshape simulation

For understanding the dynamic nature of variable temperature, static $^{13}C$ ssNMR spectra, a semiclassical exchange formalism [27] was incorporated to simulate the spectral characteristics associated with motons of the tetraalkylammonium ions. Anisotropic lineshapes of $^{13}C$ sites in $TMA^+$, $TEA^+$, $TPA^+$, and $TBA^+$ ions, which possess a tetrahedral local symmetry at the center of the molecule, that potentially undergo local $C_2$, $C_3$, or tetrahedral jumps or tumbling motions [28] have been simulated. An expression describing the $^{13}C$ CSA and $^{13}C$–$^{14}N$ dipolar interactions required for the calculation of $^{13}C$ ssNMR frequencies [29] of our sample system is given by:

$$\omega(m_s) = \left[\delta_{iso} + R^{CSA}_{2,0}\right]\omega_0 + 2R^{D}_{2,0}m_s, \tag{1}$$

where $\omega_0$ is the Larmor frequency of $^{13}C$, $\delta_{iso}$ is the orientation-independent isotropic $^{13}C$ chemical shift, $R^{CSA}_{2,0}$ and $R^{D}_{2,0}$ the orientation-dependent CSA and dipolar tensors, respectively, expressed in the spherical tensor representation, and $m_s$ the nuclear spin state of $^{14}N$ which is 1, 0, or −1. Eq. (1) can be used for calculating the NMR frequencies and the effect of chemical exchange, provided that the spatial components of the $^{13}C$ CSA and $^{13}C$–$^{14}N$ dipolar tensors of all the interconverting sites are expressed simultaneously in a common reference frame. The spatial part of the tensors, $R^{\lambda}_{2,0}$ ($\lambda$ = CSA or D), defined in the laboratory frame (LAB) can be related to the corresponding tensor elements defined in the principal axes frame (PAF), $\rho^{\lambda}_{2,\pm m}(m = -2,-1,\ldots,2)$, via a common molecular frame (MOF), $M^{\lambda}_{2,\pm n}(n = -2,-1,\ldots,2)$, according to

$$\rho^{\lambda}_{2,\pm m}(\mathrm{PAF}) \xrightarrow{(\alpha,\beta,\gamma)} M^{\lambda}_{2,\pm n}(\mathrm{MOF}) \xrightarrow{(\phi,\theta,0^\circ)} R^{\lambda}_{2,0}(\mathrm{LAB}), \tag{2}$$

where $(\alpha, \beta, \gamma)$ denotes Euler angles specifying the tensor transformation from the PAF to the MOF. In addition, $(\phi, \theta, 0^\circ)$ is a common, powder angle set specifying a transformation from the MOF to the LAB, which must be integrated over the solid sphere in order to sample the random orientations of sample molecules with respect to the external magnetic field $B_0$. The actual transformation in Eq. (2) can be carried out in terms of the second-rank Wigner rotation matrices according to

$$R^{\lambda}_{2,0} = \sum_{n=-2}^{2} d^{2}_{n,0}(\theta) \sum_{m=-2}^{2} e^{-im\alpha} d^{2}_{m,n}(\beta) e^{-in(\gamma+\phi)} \rho^{\lambda}_{2,m} \tag{3}$$

where, the CSA tensor elements are defined by $\rho^{CSA}_{2,0} = \delta_{csa}$, $\rho^{CSA}_{2,\pm1} = 0$, and $\rho^{CSA}_{2,\pm2} = \delta_{csa}\eta/\sqrt{6}$, and the dipolar tensor elements by $\rho^{D}_{2,0} = D_{zz}, \rho^{D}_{2,\pm1} = 0$, and $\rho^{D}_{2,\pm2} = 0$, respectively, in the PAF. The magnitude of the CSA tensor elements in the PAF is defined by $\delta_{csa} = \delta_{zz} - \delta_{iso}$ and $\eta = (\delta_{yy} - \delta_{xx})/\delta_{csa}$, where $|\delta_{zz} - \delta_{iso}| \geq |\delta_{xx} - \delta_{iso}| \geq |\delta_{yy} - \delta_{iso}|$ and $\delta_{iso} = (\delta_{xx} + \delta_{yy} + \delta_{zz})/3$. The magnitude of the dipolar vector in the PAF, $D_{zz}$, is provided by $(\mu_0\hbar/4\pi)(\gamma_i\gamma_j/r^3_{ij})$, where $r_{ij}$ designates the interatomic distance between atoms i and j whose magnetogyric ratios are given by $\gamma_i$ and $\gamma_j$, respectively, and $\mu_0$ is the permeability constant ($4\pi \times 10^{-7}$ kg m s$^{-2}$ A$^{-2}$). For a directly bonded $^{13}C$–$^{14}N$ site in a tetraalkylammonium ion, the strength of a $^{13}C$–$^{14}N$ dipolar coupling is $D_{zz} \approx 700$ Hz ($r$(C–N) ≈ 1.4 Å). In this simulation, we assumed a coinciding $^{13}C$–$^{14}N$ dipolar vector with respect to the $^{13}C$ CSA tensor for simplicity ($\alpha = \beta = \gamma = 0^\circ$).

Multiple exchanging sites will thus be defined by multiple $(\alpha_j, \beta_j, \gamma_j)_{1\leq j\leq N}$ sets of Euler angles. For sites undergoing $C_2$, $C_3$ or tetrahedral jumps, angle sets needed for achieving a full exchange averaging are [29,30]:

$$(\alpha,\beta,\gamma) = \begin{cases} (0^\circ, \beta, 0^\circ) \\ (0^\circ, \beta, 180^\circ) \end{cases}, \ \beta \text{ is in an arbitrary angle} \tag{4}$$

for $C_2$,

$$(\alpha,\beta,\gamma) = \begin{cases} (0^\circ, 125.3^\circ, 0^\circ) \\ (120^\circ, 125.3^\circ, 0^\circ) \\ (240^\circ, 125.3^\circ, 0^\circ) \end{cases} \tag{5}$$

for $C_3$, and

$$(\alpha,\beta,\gamma) = \begin{cases} (315^\circ, 54.7^\circ, 240^\circ) \\ (225^\circ, 125.3^\circ, 150^\circ) \\ (135^\circ, 54.7^\circ, 150^\circ) \\ (45^\circ, 125.3^\circ, 240^\circ) \end{cases} \tag{6}$$

for tetrahedral jumping, respectively.

Stochastic jumps of molecules or molecular segments occurring between these sites result in exchanging local fields of nuclear sites. This dynamic effect can be admixed into the NMR spectral calculation of sites, which is simply provided by Eq. (1) when the motion among these sites is negligible, via kinetic modifications of Bloch's equation [31] as shown below. The complete magnetization vector in the equation of motion for describing jumping motions among chemically and/or magnetically inequivalent sites can be written as [27,29,30,32,33]:

$$\frac{d}{dt}M(t) = (i\varpi + \overline{\pi})M(t). \tag{7}$$

Here, $\overline{\pi}$ defines a matrix describing the topology and the rates ($\kappa$s) of a jumping process, $\varpi$ is a diagonal matrix with elements $\omega_j(m_s) + i/T_{2j}$, where, $\omega_j(m_s)$ is the classical precessional frequency of each exchanging site provided in Eq. (1), and $T_{2j}$ is the respective transverse relaxation time. Eq. (7) can be formally solved as:

$$M(t) = \left[U\exp(\lambda t)U^{-1}\right]M_{eq} \quad (8)$$

where $M_{eq}$ is a column vector describing the equilibrium population of each site at $t = 0$, and $U$ and $\lambda$ are the eigenvectors and eigenvalues of the $(i\varpi + \overline{\pi})$ matrix, respectively. Addition of $M(t)$s over all $m_s$ values and over all the powder orientations followed by Fourier transform provide a motionally averaged exchange spectrum at a particular topology and jumping rate.

## 3. Results and discussion

Fig. 2 compares variable temperature, $^{13}C$ static CP ssNMR spectra of tetraalkylammonium ions in $TMA^+$– and $TEA^+$–form PFSIs measured at 24 °C, 40 °C, 80 °C, 120 °C, 160 °C, and 190 °C. The spectral lineshapes of these spectra provide a means to monitor the motional dynamics of these ions within the ionic domains, which are strongly influenced by the packing order and the strength of ionic interactions. In these spectra, the $^{13}C$ linewidths of the methyl and methylene groups of $TMA^+$ and $TEA^+$ ions show remarkably narrower linewidths than that of $TPA^+$ or $TBA^+$ ions (vide infra) throughout the temperatures investigated. The smaller magnitude of the observed chemical shift anisotropy (CSA) might be correlated to the stronger ordering of $TMA^+$ and $TEA^+$ ions in the ionic domains because the smaller $TMA^+$ and $TEA^+$ ions make stronger Columbic interactions with sulfonyl groups than those bulkier $TPA^+$ and $TBA^+$ ions in the ionic domains. This interpretation matches well with the observed melting points from our differential scanning calorimetry (DSC) experiments—the melting temperatures of $TMA^+$–, $TEA^+$–, $TPA^+$–, and $TBA^+$–PFSI ionomers are 253 °C, 187 °C, 123 °C, and 66 °C, respectively (data are not shown). The remarkably higher melting temperatures observed in $TMA^+$– and $TEA^+$–PFSIs are probably due to the existence of local crystalline-like ordering of $TMA^+$ and $TEA^+$ ions in the ionic domains. Interestingly, the spectral linewidths of the spectra of $TMA^+$ and $TEA^+$ ions measured at 40 °C, 80 °C, and 120 °C are somewhat broader than those measured at room temperature or temperatures above 120 °C. This slight peak broadening effect is not understood at this point. It should be pointed out that this phenomenon occurred at temperatures that are well below the $T_g$ of main chain of polymers, which are 130 °C and 110 °C for the $TMA^+$– and $TEA^+$–PFSIs, respectively.

Fig. 3 compares static $^{13}C$ CP NMR spectra of $TPA^+$ and $TBA^+$ ions in $TPA^+$– and $TBA^+$–PFSIs measured at 24 °C, 40 °C, 80 °C, 120 °C, 160 °C, and 190 °C. At temperatures in the range of 24–120 °C, the $^{13}C$ spectra of $TPA^+$ and $TBA^+$ ions exhibit broader linewidths than those of $TMA^+$ and $TEA^+$ ions, resulting in unresolved $^{13}C$ peaks among various carbon sites, except for the methylene groups that are adjacent to the nitrogen atoms. The increased CSAs of the $^{13}C$ sites in $TPA^+$ and $TBA^+$ ions might be resulted from the decreased packing order of these bulkier ions in ionic domains because of their less tightly bound nature to sulfonyl groups compared to the smaller $TMA^+$ and $TEA^+$ ions, and/or the less favorable segmental motions of alkyl arms of these ions due to the increased steric hindrance in the ionic domains. Interestingly, the $^{13}C$ spectra of $TPA^+$ and $TBA^+$ ions acquired at higher temperatures, 160 and 190 °C, demonstrate motionally averaged sharp peaks, while providing resolved peaks of all carbon sites in $TPA^+$ and $TBA^+$ ions in the spectra. This line-narrowing effect is probably resulted from the onset of overall molecular tumbling/jumping motions of $TPA^+$ and $TBA^+$ ions under high temperatures above the α-relaxation temperature. After the onset of molecular tumbling motions above the α-relaxation temperature (the α-relaxation temperatures of $TPA^+$– and $TBA^+$–PFSIs are 130 °C and 100 °C, respectively), $TPA^+$ and $TBA^+$ ions become more independent from the Columbic restraint of the sulfonyl groups of PFSIs because the onset of the thermal tumbling motions may remarkably counterbalance the force field of the electrostatic interactions—the bulkier $TPA^+$ or $TBA^+$ ions have considerably weaker electrostatic interactions with sulfonyl groups than that of either $TMA^+$ or $TEA^+$ ions. As we have seen in Fig. 2, the $TMA^+$– and $TEA^+$ ions do not demonstrate this behavior in the same temperature range probably because $TMA^+$ and $TEA^+$ ions are bound more tightly to sulfonyl groups, resulting in higher α-relaxation temperatures. It

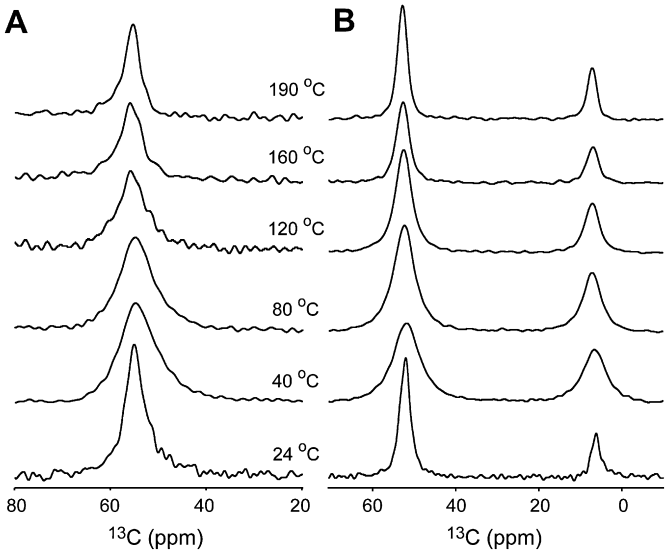


**Fig. 2.** Experimental static $^{13}C$ CP NMR spectra of $TMA^+$–PFSI (A) and $TEA^+$–form (B) PFSI membranes over the temperature range of 24 °C–190 °C. Note the slight line broadening effect around 40 °C–80 °C which can be related to a thermal disordering phenomenon.

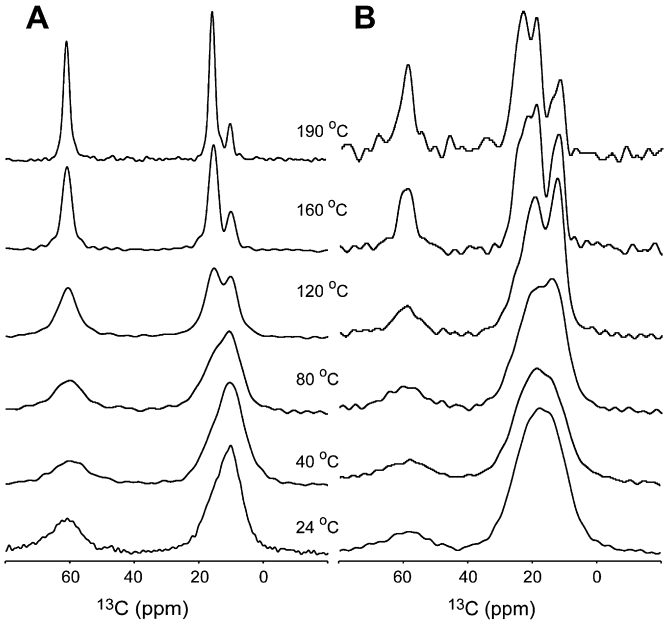


**Fig. 3.** Experimental static $^{13}C$ CP NMR spectra of $TPA^+$–PFSI (A) and $TBA^+$–PFSI (B) membranes over the temperature range of 24 °C–190 °C. A motionally averaged line-narrowing effect observed in these sample systems can be related to the tetrahedral jump/hop motions of the tetraalkyl ammonium ions at elevated temperatures, particularly at 190 °C which is well above the α-relaxation temperatures of these sample systems.

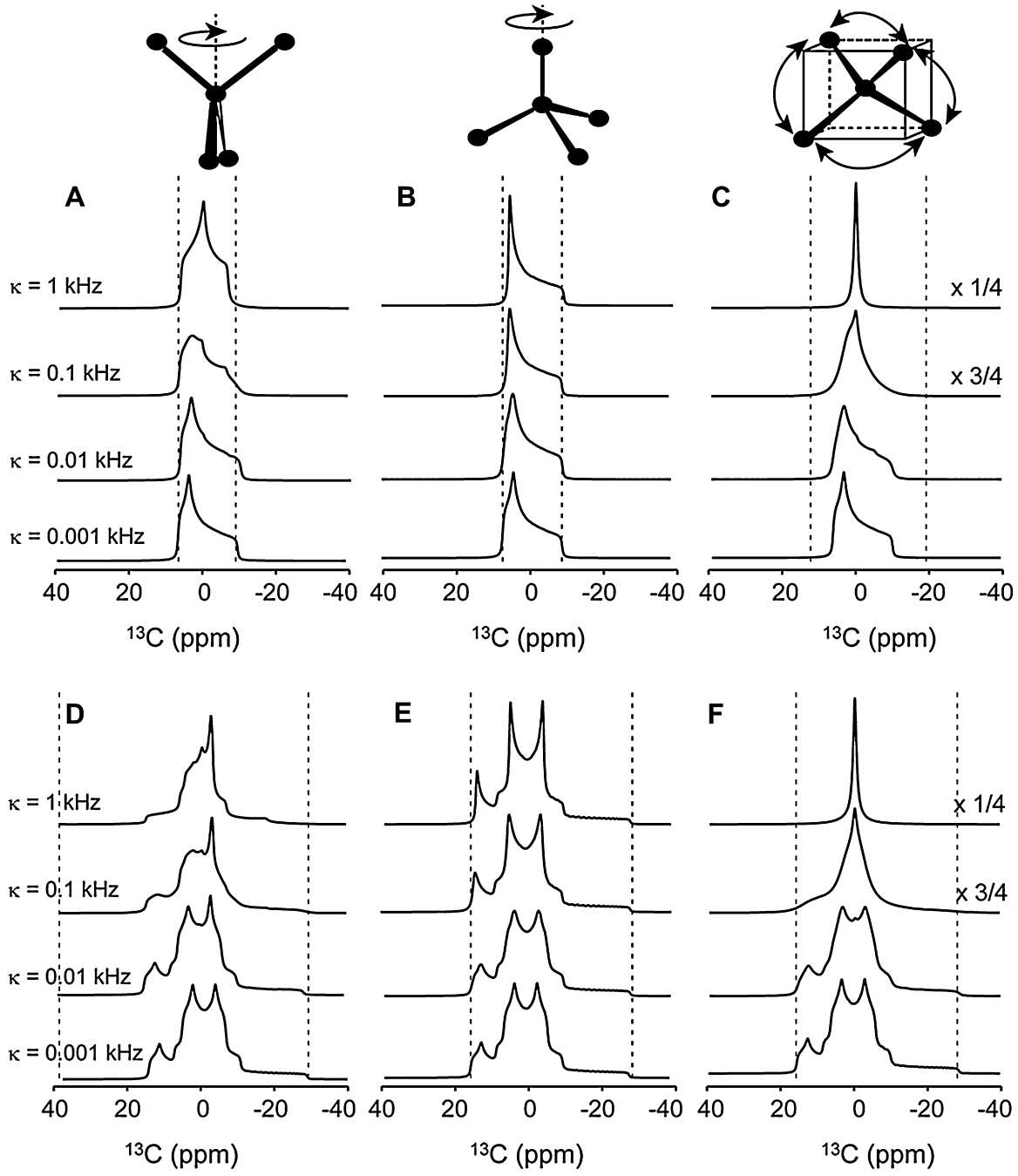


**Fig. 4.** Simulated CSA powder lineshapes of a $^{13}C$ site, with (E–F) and without (A–C) considering $^{13}C$–$^{14}N$ dipolar interaction, undergoing random $C_2$ (A and D), $C_3$ (B and E), and tetrahedral jumps/hops (C and F) with variable jump/hop rates of $\kappa = 1$, 0.1, 0.01, and 0.001 kHz. The CSA tensor parameters considered in the simulations are $\delta = 10$ ppm and $\eta = 0.3$. A 700 Hz of the coupling strength for the directly bonded $^{13}C$–$^{14}N$ dipolar pair was considered additionally in D–F. The Larmor frequency of $^{13}C$ is 75 MHz. While a site undergoing a $C_2$ or $C_3$ rotation jump/hop motion results in a motionally averaged tensor with reduced linewidth (A, B, D, and E), a $^{13}C$ site undergoing a fast tetrahedral jump/hop motion provides a motionally averaged isotropic peak (C and F).

must be noticed that the $\alpha$-relaxation temperature of the $TMA^+$–PFSI system is 230 °C which is even beyond the test range of our current temperature setting. Because the β-relaxation temperatures of both $TPA^+$– and $TBA^+$–PFSIs are lower than that of the $TMA^+$– and $TEA^+$–PFSIs, a similar type of peak broadening effect would be observed in $TPA^+$– and $TBA^+$–PFSI systems at temperatures near or lower than 40 °C or 60 °C. Although the linewidth of $TPA^+$ ions measured at 40 °C is somewhat broader than the one measured at 24 °C, the step of our temperature variation might be too big to observe this effect for the $TBA^+$–PFSI system.

To understand the fundamental characteristics of the onset of the molecular tumbling motions of tetraalkylammonium ions, we carried out theoretical simulations of $C_2$, $C_3$, and tetrahedral jumping motions that a tetraaalkylammonium ion can potentially undergo with a variable jumping rate according to the procedure described in the theoretical section. Fig. 4 shows the calculated lineshapes of a $^{13}C$ site, possessing a CSA tensor ($\delta_{CSA} = 10$ ppm; $\eta = 0.3$) and a $^{13}C$–$^{14}N$ dipolar coupling vector (d ($^{13}C$–$^{14}N$) = 700 Hz, assuming coinciding dipolar and CSA tensor orientations), undergoing $C_2$ (A and D), $C_3$ (B and E), and tetrahedral (C and F) jumps with various jumping rates, with (D, E and F) and

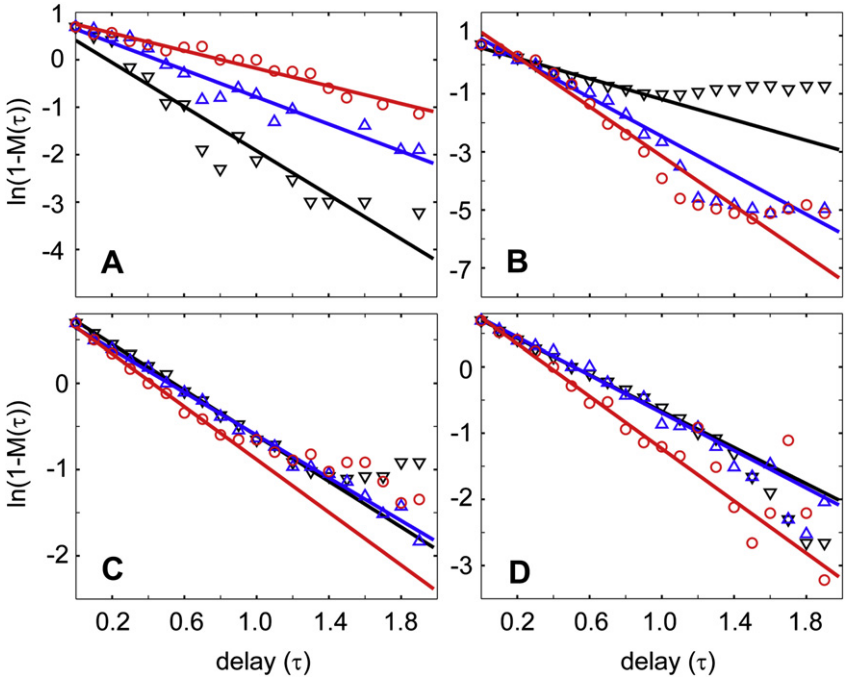


**Fig. 5.** Temperature dependence of $T_1$ relaxation times measured on the methylene or methyl protons, which are closest to the nitrogen atom, of tetraalkylammonium ions bound to PFSI ionomers. Experimentally obtained (symbols) and best-fit (lines) $^1$H $T_1$ relaxation data of $TMA^+$– (A), $TEA^+$– (B), $TPA^+$– (C), and $TBA^+$–form (D) PFSIs are shown over variable temperatures. Symbols represent experimental data at 24 °C (black circle), 120 °C (blue triangle), and 190 °C (inverted red triangle), respectively, and lines represent the best-fit curves at 24 °C (black lines), 120 °C (blue lines), and 190 °C (red lines), respectively. A formula $\ln[1 - M(\tau)] = \ln 2 - \tau/T_1$, where $\tau$ and $M(\tau)$ are a delay time and the longitudinal magnetization measured at $\tau$, respectively, is used for the curve fitting. From the slope of the curve we obtain $-1/T_1$. We considered a portion in the graph demonstrating an initial slope, experimental data with delay times less than 1.0 s, for the curve fitting when a graph exhibited multi-exponential $T_1$ behavior (For interpretation of the references to colour in this figure legend, the reader is referred to the web version of this article).

without (A, B and C) considering $^{13}C$–$^{14}N$ dipolar coupling strength. As demonstrated in Fig. 4, regardless whether the $^{13}C$–$^{14}N$ dipolar coupling is considered or not, only the tetrahedral jumping mode is capable of providing a motionally averaged, sharp line at a rate of $\kappa = 1000$ Hz or above. As compared to the spectra shown in Fig. 3, this prediction matches reasonably well with the experimental spectra of $TPA^+$ and $TBA^+$ ions observed at 160 and 190 °C, regardless whether a carbon site is adjacent to or away from the nitrogen atom. Based on these observations, it can be inferred that $TPA^+$ and $TBA^+$ ions exhibit random, rapid tetrahedral jumping/tumbling motions at a temperature well above the $\alpha$-relaxation temperature, at which tetraalkylammonium ions in the ionic domains effectively overcome the constraints of the ionic interactions. Unlike the simulated CSA/dipolar lineshapes that are obtained assuming a sample state of microcrystalline powders, the experimental spectra measured on the actual samples provide ill-defined random powder lineshapes because of the amorphous nature of the sample's morphology. Page and coworkers have reported that tetraalkylammonium ions in PFSIs make translational hopping motions at an elevated temperature above the $\alpha$-relaxation temperature based on the previous SAXS analysis [10]. In ssNMR spectra the observed line-narrowing effect evidences rotational tumbling/jumping motions of tetraalkylammonium ions. These rotational motions evidenced in ssNMR spectra provide complementary information to the SAXS data, which provide information of translational hopping motions of molecules indirectly.

Fig. 5 shows the $^1$H $T_1$ relaxation data of methylene or methyl groups that are adjacent to the nitrogen atoms of tetraalkylammonium ions in $TMA^+$–(A), $TEA^+$–(B), $TPA^+$–(C), and $TBA^+$–form PFSIs (D) at 24 °C, 120 °C, and 190 °C. When the observed data are correlated to the variable delay time, $\tau$, in a plot according to a formula $\ln[1 - M(\tau)] = \ln 2 - \tau/T_1$, where $M(\tau)$ is the measured magnetization at a variable delay time $\tau$, a straight line yielding a slope and an intercept of $-1/T_1$ and ln 2, respectively, is expected if a $T_1$ relaxation is governed by a single exponential function of time $e^{-\tau/T_1}$. $TPA^+$ (C) and $TBA^+$ (D) ions provide shorter $T_1$ times as the temperature increases. This means that ions constrained in ionic domains of ionomeric matrix undergo faster molecular collisions and therefore experience more frequent energy exchange with lattice at higher temperatures (shorter correlation times). Thus, it is natural that tetraalkylammonium ions with increased thermal energy loose their rf-induced energy states faster to the surrounding lattice, resulting in a decrease in $T_1$ [33]. Interestingly, however, the methyl protons in $TMA^+$ of $TMA^+$–form PFSI (A) show the opposite behavior; that its $T_1$ relaxation time increases as the temperature increases over the range 24–190 °C. In general, warming the sample makes the fluctuations of molecules or molecular skeletons faster, reducing the correlation time. One possibility is that the observed $T_1$ behavior would simply correspond to the case involving an opposite regime with a short correlation time, in which $T_1$ increases as temperature increases—a common $T_1$ behavior of small organic molecules dissolved in a non-viscous solvent [33]. But it is very difficult to postulate the existence of a non-viscous, solution-like environment around $TMA^+$ ions that

**Table 1**
$^1$H $T_1$ relaxation times of tetraalkylammonium ions[a] in PFSI ionomers neutralized by tetraalkylammonium ions.

| Temperature | $TMA^+$[b]–PFSI | $TEA^+$–PFSI | $TPA^+$–PFSI | $TBA^+$–PFSI |
|---|---|---|---|---|
| 24 °C | 0.43 s | 0.57 s | 0.76 s | 0.73 s |
| 120 °C | 0.70 s | 0.30 s | 0.81 s | 0.70 s |
| 190 °C | 1.08 s | 0.23 s | 0.65 s | 0.51 s |

[a] $T_1$ relaxation times of methylene or methyl groups that are directly bonded to nitrogen are recorded although other protons also exhibited $T_1$ values in the similar range, probably due to an exchange process established by $^1$H-$^1$H spin diffusion.

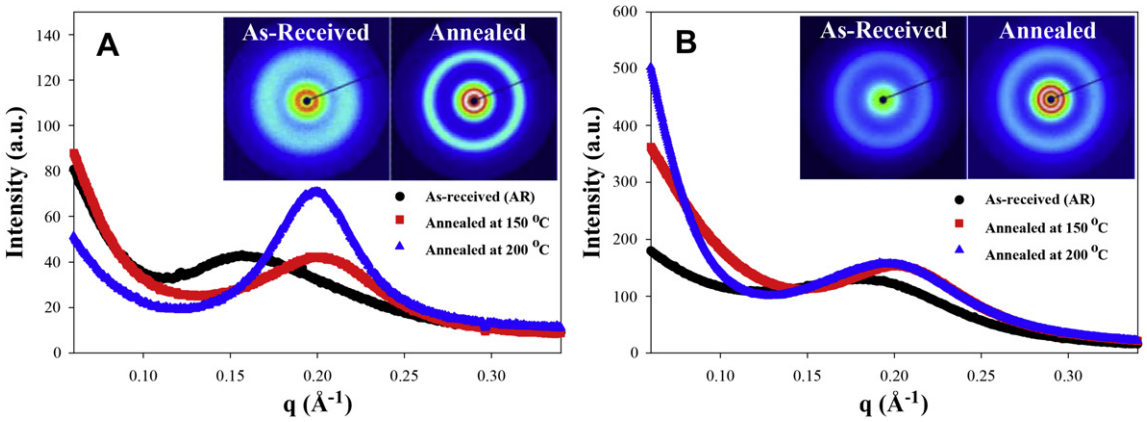


**Fig. 6.** Small-angle X-ray scattering (SAXS) profiles of $TMA^+$ (A) and $TBA^+$–Nafion (B) subjected to thermal annealing at 100 and 200 °C for 10 min. Each plot contains two-dimensional SAXS images before (left) and after (right) thermal annealing at 200 °C.

are bound in the ionic domains of solid-state PFSI ionomers. Moreover, a small $TMA^+$ ion binds more tightly to a sulfonate group in the ionic domain of PFSI than those bulkier $TEA^+$, $TPA^+$, or $TBA^+$ ions. One plausible explanation, which receives an indirect support from a small-angle X-ray scattering (SAXS) experiment that will be discussed below, is that the observed trend in $T_1$ evidences a thermally induced molecular ordering effect of $TMA^+$ ions in the ionic domains. Individual ions or smaller ionic domains of $TMA^+$s scattered around polymer matrix under low temperature can conglomerate into a bigger ionic domain by thermal annealing because smaller $TMA^+$ ions which interact strongly with sulfonyl groups can easily be accommodated into a well packed array of $TMA^+$ ions in an ionic domain. Under this situation, the portion of $TMA^+$ ions colliding with neighboring polymer matrix or segments of molecules other than $TMA^+$ ions themselves decreases as the size of ionic array increases, therefore, $TMA^+$ ions can maintain their rf-induced energy identities longer, resulting in an increase in $T_1$ time.

The $TEA^+$–form PFSI system (B) demonstrates an intermediate response between these two extreme cases discussed above. The $T_1$ curve of $TEA^+$–PFSI system shows a clear deviation from a straight line at each temperature—a probable bi-exponential $T_1$ decay behavior. Currently, this behavior is not clearly understood, but perhaps the two opposite tendencies of having faster molecular tumbling and thermal ordering at higher temperature might contribute simultaneously. For the best-fit curve fitting of a $T_1$ relaxation time we have used only the initial trend in each curve. Table 1 summarizes $^1H$ $T_1$ relaxation times of alkylammonium ions of $TMA^+$–, $TEA^+$–, $TPA^+$–, and $TBA^+$–PFSI ionomers measured at 24 °C, 120 °C, and 190 °C.

In addition to ssNMR experiments, we have performed SAXS experiments on $TMA^+$ and $TBA^+$–form PFSI membranes to further explore the possibility of thermal ordering of the aggregated counterions. Fig. 6 shows SAXS profiles of $TMA^+$–Nafion® (A) and $TBA^+$–Nafion® (B) subjected to thermal annealing at 150 °C and 200 °C for 10 min and then cooled to room temperature prior to SAXS experiment. The insets in Fig. 6 also show 2-dimensional SAXS patterns comparing before (left) and after (right) thermal annealing at 200 °C, for each countetrion form. A diffuse and broad scattering halo of maximum intensity at ca. $q = 2\ nm^{-1}$ can be observed for both $TMA^+$ and $TBA^+$ PFSI membranes and is attributed to scattering from the ionic aggregates dispersed in the ionomer matrix. While ssNMR probes directly how counterions (thus, strictly ionic domains) behave under the thermal stimulation, SAXS offer the ability to characterize phase homogeneity of the ionic and hydrophobic domains by comparing the relative sharpness of the ionomer peak. As $TBA^+$–Nafion® (Fig. 6B) is annealed at 150 °C for 10 min, the ionomer peak shifts slightly to higher $q$ with a relatively constant peak width. Annealing at even higher temperature, 200 °C (beyond the $\alpha$-relaxation temperature of $TBA^+$–form) does not seem to modify the SAXS profile significantly, except for the low $q$ region that is influenced by changes in the crystalline order of the PTFE segments of the ionomer [1,5]. For $TMA^+$–Nafion® (Fig. 6A), annealing at 150 °C for 10 min also causes the ionomer peak to shift to higher $q$ as observed in $TBA^+$–form Nafion®. However, thermal annealing at 200 °C induces a profound change in the scattering pattern. The diffuse scattering ring observed for the as-received (low temperature) state is transformed into a very distinct scattering ring with a much narrower peak width (Table 2). A greatly reduced width in the ionomer peak after thermal annealing simply means that the distribution of the ionic domain separations became narrower most likely due to the improved counterion packing order within the ionic domains. It is postulated that some of the ionic clusters become more well-ordered ones by losing loosely held interfacial ions from the aggregates or by incorporating lone ion-pairs into a bigger ionic aggregates.

Our observation is also in line with the previous ionomer annealing studies carried out by other groups utilizing ssNMR experiments. O'Connell et al. employed $^{23}Na$ ssNMR to investigate $Na^+$ neutralized sulfonated polystyrene ionomers under thermal stimulation [34]. They observed that the center of the gravity of $Na^+$ peaks had shifted to upfield from about −17 ppm to −23 ppm at thermal treatment at 160 °C for 24 h. They attributed this shift to a thermally induced ordering of $Na^+$ ions in ionic aggregation domain, most likely by the loss of loosely held interfacial ions from the aggregates. Nosaka et al. have focused on $^1H$ NMR signals of water confined in the PFSIs as a function of annealing temperatures [35]. Interestingly, the initially observed broad $^1H$ NMR spectra at 297 K were strongly affected by the thermal annealing at 358 K,which lead to a decreased line width to about one-third of that of the sample before the thermal annealing. Based on this observation, they suggested that thermal annealing provided an increased homogeneity in the chemical environments of water molecules. These NMR studies demonstrate that thermal annealing

**Table 2**
Full width at half maximum (FWHM) of the ionomer peaks for $TMA^+$–, and $TBA^+$–form Nafion®.

| Temperature | $TMA^+$–PFSI | $TBA^+$–PFSI |
|---|---|---|
| 24 °C | 0.0876 | 0.0853 |
| 150 °C | 0.0754 | 0.0765 |
| 200 °C | 0.0571 | 0.0826 |

can have a significant effect on the state of ionic aggregation in Nafion®, and our SAXS results confirm that depending on counterion type, the morphological changes can apparently involve short and long-range ordering in the ionic domains. This interesting phenomenon will be the subject of future studies.

Based on the clear ordering effect observed in the SAXS data of Fig. 6A and the supporting NMR experimental data carried out by other groups on the related compounds, we thus attribute the abnormal $T_1$ behavior of the ionomer peak observed in the $TMA^+$–form PFSI samples to a thermally induced ordering in the packing of $TMA^+$ ions in ionic domains of the PFSIs. The small $TMA^+$ ions would be suitable for producing efficiently packed ionic multiplets due to their compact size and rigid structure, and much stronger electrostatic interactions between ion-pairs [36]. One may need more experimental evidences to understand the detailed mechanism why the $TMA^+$–form PFSI system shows thermal ordering effect under an elevated temperature. We hypothesize that the strongly associated nature of $TMA^+$–PFSI system makes rotational tumbling or translational hopping movements of $TMA^+$ ions unfavorable. Instead, smaller $TMA^+$ ions may fill up gaps occurring when the polymeric matrices undergo thermally induced movements, resulting in the reinforcement of the integrity of the electrostatically aggregated states between cationic $TMA^+$ ions and anionic PFSI ionomers. Then, a $TMA^+$ ion confined more tightly in an electrostatically aggregated domain under elevated temperature would end up with a longer spin-lattice relaxation time. This may also explain why the α-relaxation temperature of the $TMA^+$–form PFSI system is much higher than those from $TEA^+$–, $TPA^+$– and $TBA^+$–form PFSIs. Reorganization of the ionic domains toward the increased order by incorporating the $TMA^+$ ions may give us a clue to design/process the novel membrane with high performance, such as proton conductivity, water diffusion, and fuel cell performance. Indeed, we have observed greatly improved fuel cell performance based on the thermally-stimulated $TMA^+$–Nafion® and these results will be published in the near future.

## 4. Conclusion

Variable temperature $^1H$ and $^{13}C$ ssNMR spectroscopy has been incorporated to study the thermally induced transitions of PFSI ionomers neutralized by tetraalkylammonium ions by observing $T_1$ relaxation times and CSAs of methyl or methylene groups in tetraalkylammonium ions. For PFSIs neutralized to contain bulkier $TPA^+$- and $TBA^+$-counterions, thermally induced ionic tumbling behaviors were observed at temperatures above the α-relaxation temperature, indicating the occurrence of a significant destabilization in the electrostatic network between sulfonyl groups and alkylammonium ions [17]. According to our simulations, the molecular tumbling motions of alkylammonium ions observed in $TPA^+$– and $TBA^+$–form PFSI complexes correspond to tetrahedral jumping with rate constants $\kappa \approx 1$ kHz. Interestingly, the $TMA^+$–form PFSI system demonstrated a dramatic increase in the $^1H$ $T_1$ relaxation time of the methyl groups in $TMA^+$ ions over the temperature range we employed, indicating that a type of thermally induced ordering effect is present even before the α-relaxation temperature. A similar type of thermally induced, molecular ordering effect had been observed in $^{19}F$ $T_1$ relaxation times, regardless of the position of $^{19}F$ nuclei in the main- or side-chains, measured over temperature ranges 25–250 °C [12]. The effects of thermal stimulation were also investigated with SAXS techniques. Depending on the type of counterions used to neutralized the PFSIs, SAXS profiles were significantly modified after thermal annealing at elevated temperatures. For example, FWHM of the ionomer peak for $TMA^+$–Nafion® clearly narrowed after thermal stimulation at 200 °C while that of $TBA^+$–Nafion® ionomer peak remained relatively unchanged. Significant narrowing of the ionomer peak is another evidence of increased order within the ionic domains.

## Acknowledgment

The authors wish to acknowledge support for this work provided by the National Science Foundation, (CHE-0541764, CHE-0619382, CMMI-0707364, and CBET-0756439). The small-angle X-ray scattering experiments at PAL were supported in part by the Ministry of Science and Technology of Korea and Pohang Steel Co.

## References

[1] Mauritz KA, Moore RB. Chem Rev 2004;104:4535–85.
[2] Gierke TD, Munn GE, Wilson FC. J Polym Sci Polym Phys Ed 1981;19:1687–704.
[3] Fujimura M, Hashimoto T, Kawai H. Macromolecules 1982;15:136–44.
[4] Dreyfus B, Gebel G, Aldebert P, Pineri M, Escoubes M, Thomas M. Journal de Physique, France 1990;51:1341–54.
[5] Rubatat L, Rollet AL, Gebel G, Diat O. Macromolecules 2002;35:4050–5.
[6] Kim M-H, Glinka CJ, Grot SA, Grot WG. Macromolecules 2006;39:4775–87.
[7] Schmidt-Rohr K, Chen Q. Nat Mater 2008;7:75–83.
[8] Moore RB, Cable KM, Croley TL. J Memb Sci 1992;75:7.
[9] Eisenberg A, Hird B, Moore RB. Macromolecules 1990;23:4098–107.
[10] Page KA, Cable KM, Moore RB. Macromolecules 2005;38:6472–84.
[11] Page KA, Landis FA, Phillips AK, Moore RB. Macromolecules 2006;39:3939–46.
[12] Page KA, Jarrett W, Moore RB. J Polym Sci Part B Polym Phys 2007;45:2177–86.
[13] Phillips AK, Moore RB. J Polym Sci Part B Polym Phys 2006;44:2267–77.
[14] Spiess HW. J Chem Phys 1980;72:6755–62.
[15] Spiess HW. Adv Polym Sci 1985;66:23–58.
[16] Schmidt C, Wefing S, Blümich B, Spiess HW. Chem Phys Lett 1986;130:84–90.
[17] Pschorn U, Rössler E, Sillescu H, Kaufmann S, Schaefer D, Spiess HW. Macromolecules 1991;24:398–402.
[18] Schmidt-Rohr K, Kulik AS, Beckham HW, Ohlemacher U, Pawelzik U, Boeffel C, et al. Macromolecules 1994;27:4733–45.
[19] Schmidt-Rohr K, Spiess HW. Multidimensional solid-state NMR and polymers. San Diego: Academic Press; 1994.
[20] Kimmig M, Strobel G, Stuhn B. Macromolecules 1994;27:2481–95.
[21] Chen Q, Schmidt-Rohr K. Macromol Chem Phys 2007;208:2189–203.
[22] Holsteina P, Schelerb U, Harris RK. Polymer 1998;(39)::4937–41.
[23] Harris RK. Nuclear magnetic resonance spectroscopy. Pitman; 1983.
[24] van Rossum B-J, de Groot CP, Ladizhansky V, Vega S, de Groot HJM. J Am Chem Soc 2000;122:3465–72.
[25] Ladizhansky V, Vega S. J Chem Phys 2000;112:7158–68.
[26] Fung BM, Khitrin AK, Ermolaev K. J Magn Reson 2000;142:97–101.
[27] McConnell HM. J Chem Phys 1958;28:430–1.
[28] In NMR spectroscopy mjohmrarmomwrttemf.
[29] Mehring M. High resolution NMR in solids. Berlin: Springer-Verlag; 1983.
[30] Schurko RW, Wi S, Frydman L. J Phys Chem A 2002;106:51–62.
[31] Bloch F. Phys Rev 1946;70:460–74.
[32] Spiess HW. Dynamic NMR spectroscopy. Berlin: Springer-Verlag; 1978.
[33] Abragam A. Principles of nuclear magnetism. New York: Oxford University Press; 1961.
[34] O'Connell EM, Root TW, Cooper SL. Macromolecules 1995;28:4000–6.
[35] Nosak AY, Watanabe S, Toyoda I, Nosaka Y. Macromolecules 2006;39:4425–7.
[36] Eisenverg A, Kim J- S. Introduction to ionomers. New York: Wiley-Interscience; 1998.